PHYSICAL REVIEW B **77**, 085120 (2008)

Identification of the carbon antisite in SiC: EPR of ^{13}C enriched crystals

Pavel G. Baranov,* Ivan V. Ilyin, Alexandra A. Soltamova, and Eugene N. Mokhov
Ioffe Physico-Technical Institute, St. Petersburg 194021, Russia

(Received 28 December 2007; published 26 February 2008)

An electron paramagnetic resonance spectrum with axial symmetry along c axis, spin $S=1/2$ and strong hyperfine interaction with one carbon atom has been observed in neutron-irradiated and annealed 6*H*-SiC, ^{13}C isotope enriched. The ^{13}C concentration was defined from hyperfine structure for the negatively charged silicon vacancy. The spectrum is identified as arising from an isolated carbon atom presumably in Si position C_{Si}—carbon antisite. The unpaired spin is up to 43% localized in one pure p orbital that is directed along the c axis and 10% localized in three sp^2 hybrid orbitals, and this means that the C atom is relaxed away from Si position.

DOI: 10.1103/PhysRevB.77.085120 PACS number(s): 61.72.J−, 61.80.Fe, 76.30.Mi

I. INTRODUCTION

Silicon carbide (SiC) is a promising wide-band-gap semiconductor for applications in high-frequency, high-temperature, high-power, and radiation-resistant electronic devices.[1] The investigation of radiation defects in SiC is of great importance in view of using ion implantation and neutron transmutation for crystal doping and also of the potential application of SiC-based devices for operation in radiation surroundings.

The primary defects, which can be produced in binary compound SiC, are vacancies, interstitials, and antisites. Electron paramagnetic resonance (EPR) is one of the most informative methods for detecting of defect unpaired spins in semiconductors and for determining the electronic structure of these defects.[2] Only few primary defects, namely, the Si and C vacancies, were studied in SiC by EPR and identified due to observation of the hyperfine (HF) interaction with ^{29}Si (nuclear spin $I=1/2$, natural abundance of 4.7%) and ^{13}C ($I=1/2, 1.1\%$) nuclei,[3–8] but up to now, there is no reliable experimental information about interstitials and antisites. It should be emphasized that unique properties of the isotopes in SiC together with a possibility to control the isotope composition or even making spin-free host crystal may offer advantages in future quantum computing and information processing applications.

Antisites take place when atoms of one element occupy sublattice sites of the other element in the compound. In III-V compounds, anion antisite defects, such as As_{Ga} (GaAs) or P_{Ga} (GaP), have been identified by EPR.[9,10] Antisite defects have technological interest; for instance, the As antisite-related *EL*2 defect is used to produce semi-insulating GaAs.[11,12] In SiC, both Si and C belong to the same column of the Periodic table, but the electronegativity of C is much larger than that of Si. Therefore, one would expect that the electronic structure of defects in SiC to be similar to that in the group III-V compounds and "anion-like" carbon antisite (C_{Si}) might have electronic states in the band gap.

A low formation energy was obtained for both antisites in SiC.[13] Carbon antisite C_{Si} was found to have lower formation energy than silicon antisite Si_C. That indicates that the C_{Si} is a common defect in SiC. The theoretical predictions for energy level positions of antisites are contradictory. While the authors of Refs. 14–16 have predicted that neither Si_C nor C_{Si} has energy levels in the band gap, recent calculations have found, on the contrary, that Si_C has several levels in the band gap, whereas the levels of the C_{Si} are in the conduction band.[13]

In Ref. 17, based on the observed ^{29}Si HF structure, it was suggested that the defect *EI*6 (*Ky*3 according to Ref. 18) observed by EPR was Si_C in 4*H*-SiC. Recent EPR measurements and calculations[18,19] have shown, however, that these centers originate from C vacancy in hexagonal position and that is not consistent with the assignment of this center to a Si antisite.

To the best of our knowledge, no experimental evidence unambiguously shows the existence of C antisite in SiC. There have been a number of experimental and theoretical studies of antisite-related complex defects in SiC,[20,21] which show the importance of the problem. However, there was no unambiguous observation of the HF structure from antisite atom itself. The small natural abundance of ^{13}C isotope makes the observation of the HF lines for C_{Si} antisite and, in particular, a quantitative fit of the observed line intensity extremely difficult task. Therefore, a 6*H*-SiC sample, grown with a ^{13}C enriched precursor material, was used in this study. In order to identify the HF structure of C_{Si} antisite, we need an independent estimate of the ^{13}C concentration in the 6*H*-SiC sample. The ^{13}C concentration of 12% was defined from the HF structure for the negatively charged silicon vacancy V_{Si}^-.

In this paper, we present results from EPR study of a new paramagnetic center in ^{13}C enriched 6*H*-SiC, which is characterized by strong HF interaction with one C atom and identified as a C antisite C_{Si}. Preliminary results on the observation of the strong HF interaction and high spin density at one C atom up to 50% were published in Ref. 22.

II. EXPERIMENT

The samples used in this study were nominally undoped *n*-type 6*H*-SiC crystals: ^{13}C enriched and with natural isotope abundance. 6*H*-SiC crystals, ^{13}C isotope enriched, were grown by the sublimation sandwich technique;[23] 6*H*-SiC crystals with natural isotope abundance were grown by the sublimation sandwich technique or Lely grown. The thick-

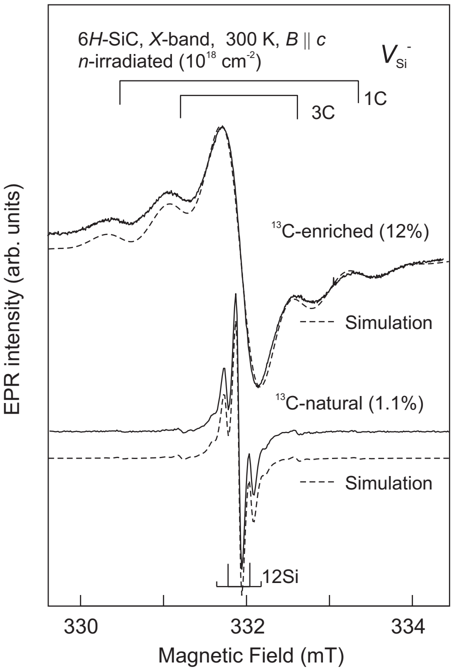

FIG. 1. EPR spectra observed in ^{13}C enriched 6*H*-SiC crystal (upper part) and 6*H*-SiC crystal with natural abundance of isotopes (lower part) for V_{Si}^{-}.

nesses of the isotope enriched crystals ranged from 0.5 to 1.0 mm. The samples were subjected to fast neutron irradiation with average energy of 1 MeV at room temperature; the neutron dose was 10^{18} cm^{-2}. After the irradiation, the isochronal annealing of the samples has been carried out. The samples have been hold at the fixed temperatures of 300°–900° with the step of 50 °C during 30 min. Then, the EPR signals have been registered at fixed low temperature. The SiC crystals investigated were cleaved in the form of a plate with known crystallographic orientation. A sample mounted in the cavity of the EPR spectrometer could be rotated in certain planes. The EPR measurements were performed using a commercial Jeol EPR spectrometer operating at a frequency of 9.3 GHz (*X* band) with a custom-made helium gas flow cryostat, which enabled the temperature to be varied within the range of 4–300 K. All EPR spectra presented in this paper are single scans (i.e., they were recorded without accumulation). Calculations of angular dependencies and a simulation of EPR spectra have been carried out using the software packages "VISUAL EPR" (written by V. Grachev) and Bruker SIMFONIA.

III. RESULTS AND DISCUSSION

Figure 1 shows *X*-band EPR spectrum observed at 300 K in *n*-irradiated ^{13}C enriched 6*H*-SiC crystal (upper part) when the magnetic field is oriented parallel to the *c* axis of the crystal ($B \| c$). A similar center was observed in 6*H*-SiC crystal with natural isotope abundance (the lower part of Fig. 1) and was attributed to V_{Si}^{-}.[4,7,8] The central line and two sets of HF lines were suggested to correspond to the isotropic HF interaction of 0.294 mT with the second-nearest-neighbor shell of the Si sites, which is composed of 12 Si atoms, and to the HF interaction with 1 and 3 C of the first shell. The set of C HF lines is anisotropic, and for the magnetic-field orientation, $B \| c$ is characterized by two doublets with splittings of 1.40 and 2.85 mT; their total intensity ratio relative to the central line is about 0.04. The two HF doublet systems correspond to the interaction with the four nearest-neighbor C atoms. There are two inequivalent sites at magnetic-field orientation $B \| c$: one site with a C atom along the *c* axis from the vacancy and the other with three C atoms at an angle of 71° of the *c* axis. The bars in Fig. 1 indicate the HF structure with 1 and 3 C of the first shell and 12 Si of the second shell for the V_{Si}^{-} vacancy in 6*H*-SiC.

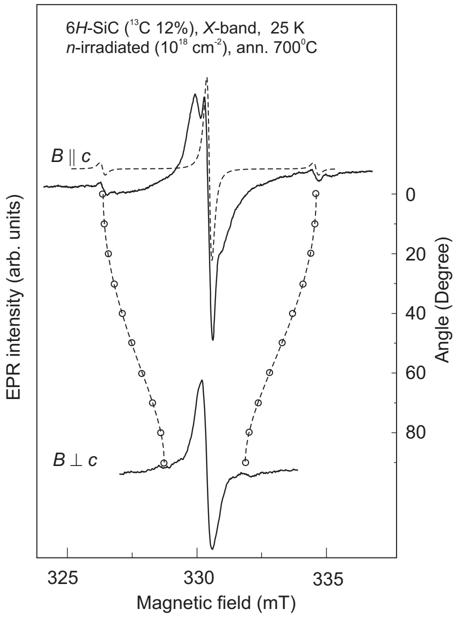

FIG. 2. Angular dependence of EPR spectra observed in *n*-irradiated and annealed ^{13}C enriched 6*H*-SiC crystal, with $P = 10$ mW and modulation amplitude of 0.1 mT.

It should be noted that in Ref. 6, the additional HF structure has been observed due to the interaction with ^{29}Si and ^{13}C atoms in the third- and fourth-nearest-neighbor shells of the Si sites, which are composed of 12 C with a splitting of 0.172 mT and 6 Si atoms with a splitting of 0.065 mT, respectively.

The apparent overall linewidth has dramatically increased from typically 0.07 in nonenriched sample to 0.5 mT in ^{13}C enriched 6*H*-SiC (Fig. 1, upper line). The dashed line in Fig. 1 (upper part) represents a simulation of the V_{Si}^{-} in ^{13}C enriched 6*H*-SiC, assuming the HF interaction with the first and the second shells as well as the interaction with 12 C atoms in the third and 6 Si atoms in the fourth shell. Taking the ^{13}C concentration as a fitting parameter, satisfactory agreement between simulation and experimental data could be achieved for a ^{13}C concentration of $12\% \pm 1\%$.

Figure 2 shows angular dependence of *X*-band EPR spectra observed at 20 K in *n*-irradiated ^{13}C enriched 6*H*-SiC crystal after 700 °C annealing. There is a strong central line and two weaker HF structure satellites symmetrically disposed on each side. The angular dependence of the HF lines

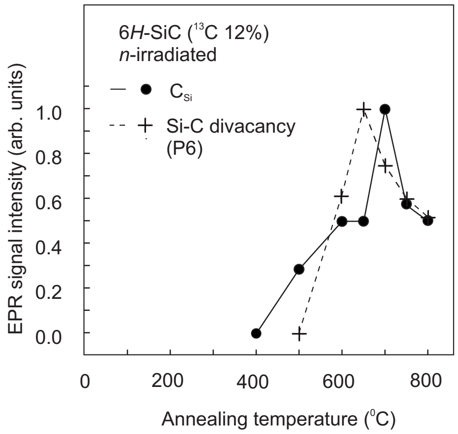

FIG. 3. The normalized intensities of the C_{Si} center and divacancy EPR signals as a function of annealing temperature for ^{13}C enriched 6*H*-SiC crystal.

measured with the magnetic field rotating in the (11−20) plane (the angle is between the direction of the magnetic field *B* and the *c* axis) is plotted as open circles. The experimental spectra are shown for $B \| c$ and for $B \perp c$. The total intensity of these two HF lines (Fig. 2) is about 12% as compared to that of the main line. This intensity ratio is approximately equal to the abundance of the ^{13}C isotope in isotope enriched 6*H*-SiC. HF satellites, reflecting the ^{13}C isotopic abundance, reveal the unambiguously incorporation of a single C atom in the defect.

The EPR spectra of the new center are described by the standard spin Hamiltonian. The angular dependence study has shown, which the HF and *g* tensors have axial symmetry along *c* axis with the HF structure constant for the interaction with one C atom $A_{\|}=8.11$ mT and $A_{\perp}=3.0$ mT; $g_{\|}=2.0045$ and $g_{\perp}=2.0055$. The theoretical angular dependence of the HF structure is shown in Fig. 2 as dashed lines.

As far as we know, these values of HF interaction are the largest interactions with one carbon atom in SiC and could be typical for antisite C_{Si} or interstitial C_i carbon atom. The observed signal is labeled as C_{Si}; the reason for this designation will be given later.

The EPR spectrum of C_{Si} center is observed in the 5−50 K temperature range. We observe a slight reduction in the HF splitting of the center in the 40−50 K range and its disappearance above 50 K. For lower temperatures, the spectrum decreases in intensity, and at 4.2 K, is no longer observable.

Figure 3 shows the normalized intensities of the C_{Si} center EPR signals as functions of annealing temperature (at each temperature, the annealing time was 30 min) for ^{13}C enriched 6*H*-SiC crystal. In addition for comparison, the data for Si-C divacancy[3,22,24,25] for the same crystal are presented. The C_{Si} center and divacancy signals are normalized to their values at annealing temperatures of 700 and 650 °C, respectively. The divacancy spectrum was detected under the illumination in order to enhance the signal due the optical alignment of the triplet spin levels in the ground state.[22] C_{Si} and divacancies demonstrate similar thermal annealing behavior.

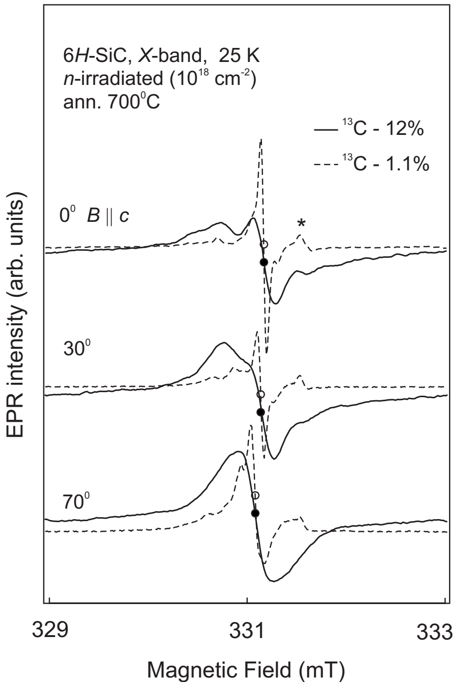

FIG. 4. The central part of EPR spectra observed in ^{13}C enriched 6*H*-SiC crystal (solid line) and 6*H*-SiC crystal with natural abundance of isotopes (dashed line) after *n* irradiation and annealing. The asterisk marks a reference signal of quartz.

The “fingerprint” of the new defect C_{Si} is a strong HF structure, since the central part of the EPR spectrum is superimposed with strong signals from other defects. Figure 4 shows the central part of the *X*-band EPR spectra observed at 20 K in ^{13}C enriched 6*H*-SiC crystal (solid line) and 6*H*-SiC crystal with natural abundance of isotopes (dashed line). In $B \| c$ orientation, the signal of the C_{Si} center is dominant for ^{13}C enriched and nonenriched 6*H*-SiC crystal. For other orientations, this signal is more overlaped with the signal of other radiation defects. This central signal belongs to the more common isotope ^{12}C (98.9%) which has nuclear spin $I=0$; thus, no HF splitting can be observed for this isotope. The positions of the central line are marked by filled and open circles for ^{13}C enriched and nonenriched crystals, respectively. The linewidth has essentially increased in ^{13}C enriched 6*H*-SiC from 0.07 to 0.2 mT due to inhomogeneous broadening by 12% ^{13}C atoms. Since the effective *g* factors are the same as those observed in nonenriched case and they have similar annealing behavior, we believe that we observe the same defect in both samples. The intensity of the HF lines due to interaction with one C atom was too low to be surely detected in nonenriched 6*H*-SiC.

Based on the observed strong ^{13}C HF interaction with one C atom, it is suggested that the defect can be either carbon antisite C_{Si} or carbon interstitial C_i. The HF interaction tensor components can be expressed in terms of the isotropic *a* and anisotropic *b* components as $A_{\|}=a+2b$ and $A_{\perp}=a-b$ with axial symmetry around the *p* function axis. Here, $a=(8\pi/3)g_e\beta_e g_n\beta_n|\Psi_{2s}(0)|^2$ and $b=(2/5)g_e\beta_e g_n\beta_n\langle r_{2p}^{-3}\rangle$, where g_e is the electronic *g* factor, β_e is the electronic Bohr magneton, g_n is the nuclear *g* factor, β_n is the nuclear magneton, and Ψ is unpaired-electron wave function.

Using the linear combination of atomic orbital analysis,[26] and by assuming that the atomic orbital of C in SiC does not

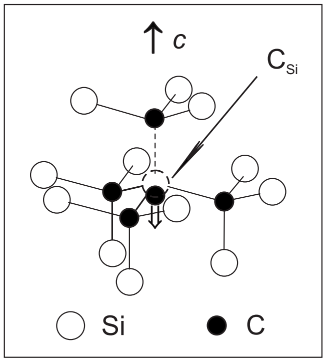

FIG. 5. The model showing a possible configuration of the carbon antisite.

differ from that of a free C atom,[27] the spin densities on C atom are determined as 3.4% on the *s* orbital and 42.8% on the *p* orbital; therefore, one has 92% of 2*p* character and 8% of 2*s* character. Thus, the fraction of *p* character is much larger than 75% as expected for a sp^3 hybrid orbital. It is useful to compare this result with a similar ^{13}C HF structure observed for the isolated interstitial carbon atom in silicon which was specially doped with carbon enriched ^{13}C isotope.[28] For this defect, 36% of the unpaired spin wave function was located on the carbon atom, which had 97% 2*p* and 3% 2*s* character.

Different inequivalent interstitial sites in 6*H*-SiC are surrounded by four or six Si atoms. Thus, the HF structure for ^{29}Si atom at four or six nearest Si neighboring sites should be observed at least in 6*H*-SiC with the natural isotope abundance similar to the case for the isolated interstitial C atom in silicon.[28] This is not observed in our case (Fig. 4). In opposite, the linewidth has increased essentially in ^{13}C enriched 6*H*-SiC compared with nonenriched cyrstal. This line broadening due to HF interaction with the nearest-neighbor ^{13}C ligands together with the central HF interaction with one ^{13}C atom strongly suggest that this center involves a C atom occupying a Si site, i.e., a C antisite C_{Si}.

The spin density is mainly localized in the p_z orbital of a carbon, which is directed along the Si-C connection line and parallel to the *c* axis. The four orbitals of carbon are suggested to be shifted from sp^3 hybrid orbitals to three sp^2 hybrid orbitals and one pure *p* orbital, in which the unpaired spin is mainly localized. It is known that threefold-coordinated atom in covalent molecules tends to go planar with sp^2 bonding.[29] The deviation of the carbon orbitals from a sp^3 hybrid configuration to a sp^2 configuration indicates the presence of a shift of the carbon atom from its central position away from Si position along the Si-C connection line. The model showing a possible configuration of the carbon antisite is illustrated in Fig. 5; the double arrow shows a shift of the C atom from its central Si position. If we assume the carbon to be in a sp^2+p configuration, the 3.4% of spin density in the *s* orbital should be shared between three sp^2 orbitals. This results in three sp^2 orbitals, with $3.4/3 = 1.13\%$ density in the *s* orbital and 2.26% in the *p* orbital. In total, without taking into account polarization effects, the spin density at one carbon is estimated to be $3(1.13+2.26)+42.8=53\%$.

Other possibility to explain the strong HF interaction is a broken carbon dangling bond. The broken C bond could be caused by an impurity or Si-vacancy related defect. For example, for the shallow B acceptor in SiC, about 35% of unpaired spin density is located on the dangling bond of a carbon atom along the C-B connection line.[30,31] We assume that the new center is intrinsic defect, since it could be detected in SiC crystals from different sources and no additional HF interactions with impurities were observed. We can also rule out a Si-vacancy related defect, since the EPR spectra of Si vacancy in different charge states were well studied.

We can estimate the spin density on the three C nearest neighbors of the carbon antisite (the model in Fig. 5) by considering the HF interaction, which could be estimated from the line broadening (Fig. 4). The observed isotropic *a* parameter of about 0.3 mT corresponds to a spin density of about 0.3% on the *s* orbital of carbon. If we assume sp^3 hybrid orbitals for each of the three nearest-neighbor carbons, the total spin density on carbon is supposed to be four times larger, i.e., 1.2% and totally 3.6%. Due to off-center position of C atom, an HF interaction with the fourth C nearest neighbor along the *c* axis is estimated to be negligible to contribute to the linewidth.

Concerning the *g* tensor, the finding, that the deviation of g_z from g_e is smaller as compared to that of $g_\perp$, supports our model, in which the unpaired electron is localized in the p_z orbital, because the expectation value of the orbital angular momentum along this direction is zero.

We consider $S=1/2$ for C_{Si}. Sometimes, it is difficult to make spin assignment for a system with lack of zero-field splitting (like it was for the negatively charged Si vacancy with $S=3/2$), but it seems to be not a case for our model with the strong HF interaction. The HF splitting is equal to $A/2S$; therefore, for *S* larger than 1/2, the spin density at C nucleus should be about or larger than 100%. The spin $S=1/2$ indicates that the charge state of the C_{Si} could be +1 or −1. Since the crystal was heavily *n* irradiated, the charge state of this defect is suggested to be positive, i.e., $C_{Si}{}^+$. In addition, the constant of the HF structure for C_{Si} antisite is about two times larger compared with that of the HF structure constant of *d*2 center in SiC, which was suggested[32] to be $(C_2)_{Si}$.

During preparation and reviewing of the paper, new results on C-antisite-related defects were published by Umeda *et al.*[33] The strong HF interaction with one C atom, comparable with that of this paper as well as with our preliminary results,[22] was observed in 4*H*-SiC crystal, electron irradiated at extremely high temperatures of 850 °C in conditions of a high mobility of the C and Si vacancies. These spectra were assigned to another state of Si vacancy (C_{Si}-V_C pair). We do not support similar model for the center observed in our papers since the decisive proof of the existence of such defect, to our mind, will be the possibility to convert (e.g., optically, by temperature or others physical influence) this defect from one state to another, like it was observed for other semiconductors. What is more, both states of Si vacancy should be detected in the crystal. To our mind, a more reasonable interpretation of the defects observed by Umeda *et al.* could be C-Si antisites pair. In spite of the difference in the properties of the centers observed by our group and by

Umeda *et al.* (different observation temperatures, different irradiation conditions, different polytypes, and different HF interactions with Si), the important result is the observation of a new type of defects with a strongly localized spin density on one C atom.

IV. SUMMARY

The EPR spectrum with axial symmetry along c axis, spin $S=1/2$ and strong HF interaction with one C atom, has been observed in neutron-irradiated and annealed 6H-SiC, ^{13}C isotope enriched. The ^{13}C concentration of 12% was defined taking the ^{13}C concentration as a fitting parameter for the simulation of HF structure for the V_{Si}^{-}. Based on the observed ^{13}C HF structures and high spin density at one C atom up to 50%, it was suggested that the defect is the isolated C, presumably in Si position–C antisite ($\mathrm{C_{Si}}$). The spin density is mainly localized in the p_z orbital of a C, which is directed along the Si-C connection line and parallel to the c axis. The four orbitals of C are suggested to be shifted from sp^3 hybrid orbitals to three sp^2 hybrid orbitals and one pure p orbital, in which the unpaired spin is mainly localized. This means that the C atom is relaxed away from Si position. The spin $S=1/2$ suggests that the C is in the positive-charge state $\mathrm{C_{Si}}^{+}$.

ACKNOWLEDGMENTS

This work was supported by the Programs of RAS Spin-Dependent Effects in Solids and Spintronics, P-03 Quantum Macrophysics, RFBR, and St. Petersburg Scientific Center.

---

*pavel.baranov@mail.ioffe.ru

[1] W. J. Choyke and G. Pensl, MRS Bull. **22**, 25 (1997).
[2] G. D. Watkins, in *Point Defects in Solids*, edited by J. H. Crowford and L. M. Slifkin (Plenum, New York, 1975), Vol. 2, p. 333–392; *Deep Centers in Semiconductors*, edited by S. T. Pantelides (Gordon and Breach, New York, 1986), pp. 147–183.
[3] V. S. Vainer and V. A. Il'in, Sov. Phys. Solid State **23**, 2126 (1981).
[4] J. Schneider and K. Maier, Physica B **185**, 199 (1993).
[5] T. Wimbauer, B. K. Meyer, A. Hofstaetter, A. Scharmann, and H. Overhof, Phys. Rev. B **56**, 7384 (1997).
[6] H. J. von Bardeleben, J. L. Cantin, I. Vickridge, and G. Battistig, Phys. Rev. B **62**, 10126 (2000).
[7] E. Sorman, N. T. Son, W. M. Chen, O. Kordina, C. Hallin, and E. Janzen, Phys. Rev. B **61**, 2613 (2000); M. Wagner, B. Magnusson, W. M. Chen, E. Janzen, E. Sorman, C. Hallin, and J. L. Lindstrom, Phys. Rev. B **62**, 16555 (2000).
[8] P. G. Baranov, E. N. Mokhov, S. B. Orlinskii, and J. Schmidt, Physica B **308-310**, 680 (2001); S. B. Orlinski, J. Schmidt, E. N. Mokhov, and P. G. Baranov, Phys. Rev. B **67**, 125207 (2003).
[9] U. Kaufmann, J. Schneider, and A. Rauber, Appl. Phys. Lett. **29**, 312 (1976).
[10] H. J. von Bardeleben and J. C. Bourgoin, J. Appl. Phys. **58**, 1041 (1985).
[11] M. O. Manasreh, D. W. Fischer, and W. C. Mitchell, Phys. Status Solidi B **154**, 11 (1989).
[12] U. Kaufmann, Mater. Sci. Forum **143-147**, 201 (1994).
[13] L. Torpo, S. Poykko, and R. M. Nieminen, Phys. Rev. B **57**, 6243 (1998) and references therein.
[14] Y. Li and P.-J. Lin-Chung, Phys. Rev. B **36**, 1130 (1987).
[15] C. Wang, J. Bernholc, and R. F. Davis, Phys. Rev. B **38**, 12752 (1988).
[16] D. N. Talwar and Z. C. Feng, Phys. Rev. B **44**, 3191 (1991).
[17] N. T. Son, P. N. Hai, and E. Janzen, Phys. Rev. Lett. **87**, 045502 (2001).
[18] V. V. Konovalov, M. E. Zvanut, and J. van Tol, Phys. Rev. B **68**, 012102 (2003).
[19] V. Ya. Bratus', I. N. Makeeva, S. M. Okulov, T. L. Petrenko, T. T. Petrenko, and H. J. von Bardeleben, Mater. Sci. Forum **353-356**, 517 (2001); V. Ya. Bratus', T. T. Petrenko, S. M. Okulov, and T. L. Petrenko, Phys. Rev. B **71**, 125202 (2005).
[20] T. Umeda, N. T. Son, J. Isoya, E. Janzen, T. Ohshima, N. Morishita, H. Itoh, A. Gali, and M. Bockstedte, Phys. Rev. Lett. **96**, 145501 (2006).
[21] Alexander Mattausch, Michel Bockstedte, and Oleg Pankratov, Phys. Rev. B **69**, 045322 (2004); A. Gali, P. Deak, P. Ordejon, N. T. Son, E. Janzen, and W. J. Choyke, *ibid.* **68**, 125201 (2003).
[22] P. G. Baranov, I. V. Il'in, E. N. Mokhov, M. V. Muzafarova, S. B. Orlinskii, and J. Schmidt, JETP Lett. **82**, 441 (2005); I. V. Ilyin, M. V. Muzafarova, E. N. Mokhov, V. I. Sankin, P. G. Baranov, S. B. Orlinskii, and J. Schmidt, Mater. Sci. Forum **527-529**, 535 (2006).
[23] Yu. A. Vodakov, E. N. Mokhov, G. Ramm, and A. D. Roenkov, Krist. Tech. **14**, 729 (1979).
[24] N. T. Son, P. Carlsson, J. ul Hassan, E. Janzen, T. Umeda, J. Isoya, A. Gali, M. Bockstedte, N. Morishita, T. Ohshima, and H. Itoh, Phys. Rev. Lett. **96**, 055501 (2006).
[25] W. E. Carlos, N. Y. Garces, E. R. Glaser, and M. A. Fanton, Phys. Rev. B **74**, 235201 (2006).
[26] G. D. Watkins and J. W. Corbett, Phys. Rev. **134**, A1359 (1964); **138**, A543 (1965).
[27] J. R. Morton and K. F. Preston, J. Magn. Reson. (1969-1992) **30**, 577 (1978).
[28] G. D. Watkins and K. L. Brower, Phys. Rev. Lett. **36**, 1329 (1976).
[29] G. G. DeLeo, W. B. Fowler, and G. D. Watkins, Phys. Rev. B **29**, 3193 (1984).
[30] A. G. Zubatov, I. M. Zaritskii, S. N. Lukin, E. N. Mokhov, and V. G. Stepanov, Sov. Phys. Solid State **27**, 197 (1985) [Fiz. Tverd. Tela (Leningrad) **27**, 322 (1985)].
[31] A. van Duijn-Arnold, J. Mol, R. Verberk, J. Schmidt, E. N. Mokhov, and P. G. Baranov, Phys. Rev. B **60**, 15829 (1999).
[32] I. V. Ilyin, M. V. Muzafarova, E. N. Mokhov, P. G. Baranov, S. B. Orlinskii, and J. Schmidt, Physica B **340-342**, 128 (2003); I. V. Ilyin, M. V. Muzafarova, E. N. Mokhov, and P. G. Baranov, Semicond. Sci. Technol. **22**, 270 (2007).
[33] T. Umeda, J. Ishoya, T. Ohshima, N. Morishita, H. Itoh, and A. Gali, Phys. Rev. B **75**, 245202 (2007).